"Incorporation of Zebularine from its 2'-deoxyribonucleoside triphosphate derivative and activity as a template-coding nucleobase." Dowd, C.L., Sutch, B.T., Haworth, I.S., Eritja, R., Marquez, V.E., Yang, A.S.Nucleosides, Nucleotides & Nucleic Acids, 27, 131-145 (2008).

Incorporation of Zebularine from its 2'-Deoxyribonucleoside Triphosphate Derivative and Activity as a Template-Coding Nucleobase

Running Title: Zebularine Incorporation into DNA

Casimir L. Dowd[1], Brian T. Sutch[2], Ian S. Haworth[2], Ramón Eritja[3], Victor E. Marquez[4], and Allen S. Yang[1,5]

[1]Department of Medicine, Keck School of Medicine, and [2] Department of Pharmaceutical Sciences, University of Southern California, Los Angeles, CA 90033
[3]Institut de Biología Molecular de Barcelona-CSIC, Jordi Girona 18-26, E-08034 Barcelona, Spain
[4]Laboratory of Medicinal Chemistry, Center for Cancer Research, National Cancer Institute at Frederick, Frederick, MD 21702
[5]To whom correspondence should be addressed: allenyan@usc.edu

Abstract

Zebularine (1-(β-D-ribofuranosyl)-1,2-dihydropyrimidin-2-one) was studied as both a 2'-deoxyribosyl 5'-triphosphate derivative and as a template incorporated into an oligonucleotide. Using a novel Pyrosequencing assay zebularine acted as cytosine analog and was incorporated into DNA with a template pairing profile most similar to cytosine, pairing with greatest efficiency opposite guanine in the template strand. Guanine was incorporated with greater affinity than adenine opposite a zebularine in the template strand. Computer modeling of base-pairing structures supported a better fit of zebularine opposite guanine than adenine. Zebularine acts as a cytosine analog, which supports its activity as an inhibitor of cytosine methyltransferase.

Abbreviations:

A: Adenine, C: Cytosine, G: Guanine, T: Thymine, dNTP: 2'-deoxynucleotide 5'-triphosphate, dZTP: 2'-deoxy-zebularine 5'triphosphate, ara-dCTP: 2'-deoxy-cytosine-β-arabinofuranoside 5'-triphosphate, 5mdCTP: 5-methyl-2'-deoxycytidine 5'-triphosphate, dUTP: 2'-deoxyuridine 5'-triphosphate

Introduction

Methylation of cytosine at CpG dinucleotides is involved in gene silencing, and aberrations in DNA methylation are well described in cancer. Aberrant de novo methylation in the regulatory sequences of tumor suppressor genes can result in their silencing and inappropriate gene regulation. This abnormal DNA methylation may lead to abnormal cell growth and tumorigenesis(1). Methylation of cytosine is catalyzed by DNA methyltransferase enzymes, all of which work through the same catalytic mechanism(2). The addition of a methyl group at the 5-position of cytosine is dependent on formation of a covalent intermediate between a conserved cysteine moiety of the enzyme and the 6-position of the cytosine ring (Figure 1A&B) (3-5). Numerous drugs have been shown to inhibit DNA methylation. The most frequently studied agents are the cytosine analogs, 5-azacytidine and 5-aza-2'-deoxycytidine, which have a nitrogen at the 5-position of the pyrimidine ring (Figure 1C). These triazine analogs are converted to their triphosphate forms by intracellular kinases and are then incorporated into DNA in place of cytosine. Once incorporated into DNA, the methyltransferase enzyme attempts to catalyze methyl transfer by forming a covalent bond at the 6-position of the azacytosine ring that prevents DNA and cofactor release (6). Thus these cytosine analogs covalently trap DNA methyltransferase during the methylation process. Such covalent trapping leads to irreversible inhibition of the enzyme, depletion of the enzyme, and an overall decrease in DNA methylation(7, 8).

Drugs that inhibit DNA methylation have demonstrated activity against cancer, especially hematologic malignancies(9, 10). Both 5-azacytidine and 5-aza-2'-deoxycytidine are used to treat myeloid hematologic malignancies(11). In vitro studies have shown that azacytidine

optimally inhibits DNA methylation in cell culture when given at low doses for prolonged periods of time, which allows for depletion of the enzyme with decreased cytotoxicity(8). Recent clinical studies have focused on the prolonged use of these drugs at low doses in order to maximize the ability to inhibit DNA methylation (12, 13). Such studies have shown that these drugs may be more active at low doses with longer periods of administration (14). Thus oral administration of a DNA methylation inhibitor may be ideal for clinical use.

Another pyrimidine analog, zebularine, which can be orally administered, has also been shown to inhibit DNA methylation (Figure 1D) (15-18). However, zebularine is approximately 30 times less potent in inhibiting DNA methylation when compared to 5-azacytidine and 300 times less potent than 5-aza-2'-deoxycytidine(15). Interestingly, once incorporated into DNA, the 2-(1*H*)-pyrimidinone base of zebularine has an equivalent or greater potency compared to azacytosine in inhibiting DNA methyltransferase(19-22). Therefore, it is postulated that zebularine is a weaker inhibitor of DNA methylation due to a lower efficiency of incorporation into DNA compared to 5-azacytidine and 5-aza-2'-deoxycytidine. Prior to incorporation into DNA, zebularine must be converted to nucleotide precursors; zebularine is initially phosphorylated by uridine/cytidine kinase to a monophosphate and then further phosphorylated into a di- and triphosphate by cellular kinases. In addition, conversion to a 2'-deoxyribonucleotide by ribonucleotide reductase is required in order for zebularine to be incorporated into DNA. In contrast, 5-aza-2'-deoxycytidine is already a 2'-deoxyribonucleoside that can be phosphorylated by deoxycytidine kinase, and is able to avoid the metabolic rate limiting step of reduction by ribonucleotide reductase(22, 23).

The ability of zebularine to inhibit DNA methylation is dependent on its capacity to efficiently incorporate in place of cytosine and act as a target for DNA methyltransferase. This Trojan horse approach can lead to covalent trapping of the enzyme by the 2-(1*H*)-pyrimidinone ring of zebularine. However, previous studies have shown that when zebularine is incorporated into the template strand of DNA, it acts as a poor cytosine analog and leads to blockage of DNA replication(24). Therefore, we hypothesized that zebularine, as its 2'-deoxy-5'-triphosphate derivative, may not be efficiently incorporated into DNA in place of cytosine, given the lack of a 4-amino group. We used a novel pyrosequencing nucleotide extension assay and computer modeling to study the incorporation of zebularine and other nucleotide analogs opposite various nucleotide templates. These studies were extended to examine incorporation of dNTPs opposite a template strand containing zebularine.

Materials and Methods

Primers and Templates

All primers and templates except the zebularine-containing oligonucleotides were synthesized by the Microchemical Core Facility at the USC/Norris Comprehensive Cancer Center using an Applied Biosystems Inc, (ABI) 3948 DNA synthesizer (Templates) or ABI 394 DNA synthesizer (Complementary sequencing primer). The template used for insertion analysis was a 30-nucleotide oligomer based on the wild-type single stranded M13 bacteriophage DNA sequence from position 1797 to 1826 with the sequence 5'-CTCAGTGTTAC**X**GTACATGGGTTCCTATTG-3' (25), in which X denotes the variable position, which was A (M13A), C(M13C), G(M13G) , T (M13T), hypoxanthine (M13I) or zebularine (M13Z) in the respective oligomers. The complementary primer used to conduct

pyrosequencing was an 18-mer with the sequence: 5'-CAATAGGAACCCATGTAC-3' (M13Comp1) (Figure 2).

Zebularine-containing oligonucleotides were prepared using an Applied Biosystems 3400 DNA synthesizer. The corresponding 5'-*O*-DMT-2'-deoxyzebularine-3'-*O*-2-cyanoethyl-*N*,*N*-diisopropylphosphoramidite (2'-zebularine phosphoramidite) was synthesised as reported (26). The oligonucleotide synthesis was performed in 3 parts: synthesis of the sequence to the 5' side of zebularine, addition of 2'-deoxyzebularine phosphoramidite (loaded at position 5 of the synthesizer), and finally synthesis of the remainder of the oligonucleotide sequence. This was done in order to use a special synthesis cycle for the addition of 2'-deoxyzebularine phosphoramidite, which required a longer coupling time. The standard bases were added using the standard LV200 synthesis cycle. Syntheses were performed without the removal of the last DMT group. 2'-Deoxyguanosine was protected with a dimethylformamidine group. Ammonia treatment was performed at 55ºC for 30 min to preserve the integrity of zebularine. Oligonucleotides were purified using reversed-phase HPLC (DMT on). The DMT was removed with 80% acetic acid and the acetic acid was removed by extraction with ethyl ether. The resulting product was desalted with Sephadex G-25 (NAP-10 column).

Nucleotides

dNTP substrates A, C, G, and T were purchased from Eppendorf (Westbury, NY. catalogue #954143023). 2'-Deoxy-5-methylcytidine 5'-triphosphate (d5mCTP) was purchased from Fermentas (Hanover, MD #RO431), as was 2'-deoxyuridine 5'-triphosphate (dUTP, #R0133). 2'-

Deoxy-cytosine -β-D-arabinofuranoside triphosphate (ara-dCTP) was purchased from Sigma (St. Louis, MO. #C-3639). 2'-Deoxy-zebularine triphosphate (dZTP) was synthesized by Trilink Biotechnologies (San Diego, CA), as previously described (27). Nucleotides were diluted from stocks to 10mM in PCR-grade water and a 1/10 serial dilution was performed to obtain the 1mM, 0.1mM and 0.01mM working concentrations.

Pyrosequencing

Pyrosequencing is a novel method of DNA sequence analysis, offering an accurate and efficient alternative to previously described radiolabeling or fluorescence based methods (28). Incorporation of a dNTP into an oligonucleotide chain by DNA polymerase and the concomitant release of pyrophosphate (PPi) initiates a multi-enzyme pathway ultimately generating detectable light (29). Light intensity is proportional to the quantity of dNTP incorporated during a constant time interval, and has been shown to be useful in quantitation of single nucleotide polymorphisms in mixed samples (30, 31). Here we adapt the method to determine the efficacy of the polymerase in incorporating various conventional and modified nucleotide triphosphates opposite to a template of known base sequence by using a standardized concentration of dNTP substrate, template and primer. We are able to extrapolate the K_m and Km/V_{max} for each dNTP by utilizing the signal intensity over a constant time interval as a surrogate for reaction velocity.

Templates (M13A, M13C, M13G, M13T, M13I and M13Z) were combined individually with M13Comp1 to a final concentration of 0.25mM for each and aliquoted in triplicate to the assay plate. Additionally an M13Comp1-only sample, as well as an M13G-only and a buffer-only control, were included to determine the signal obtained in the absence of template-specific

primer extension. The conventional 'A', 'C', 'G' and 'T' nucleotide-dispensing cartridges of the pyrosequencer were filled with either 10mM, 1mM, 0.1mM or 0.01mM of the nucleotide being assayed for that run.

Determination of Efficiency of Incorporation and Calculation of Km/V

Chemoluminescent signal generated by pyrosequencing is converted to a numerical value referred to as a "Peak Height." This value is directly proportional to the amount of dNTP substrate incorporation in a constant time interval; The peak height was used as a surrogate approximation of polymerase reaction velocity. Pyrosequencing reactions were performed in a final volume of 12 microliters and the nucleotide dispensing tips were used to inject 50nl of dNTP in each reaction from which the final concentration of dNTP was calculated for each reaction. The Km/V was estimated using a Lineweaver-Burke plot; where 1/[S (peak height)] was plotted against 1/[dNTP].

Computer Modeling

Duplexes comprising the primer and template sequences and with a single base (Y) incorporated opposite X in the template were constructed in a B-DNA conformation (with part of the template strand as an overhang) using in-house software, NASDAC (32). Structures were built with X-Y = C-Z, A-Z, G-Z, I-Z, C-G, A-T, G-C and I-C, and for the zebularine-containing template with X-Y = Z-G, Z-C, Z-A and Z-T. Minimization of each structure was performed in AMBER8 (33): following neutralization with sodium ions, the structure was minimized for 4000 cycles, using a 200Å non-bonded cutoff and a distance-dependent dielectric of 4r (using the parameter eedmeth=5). The AMBER parameters for zebularine were the same as those of cytosine, with

adjustment of charges and atom types around position 4 of the pyrimidine ring: charges for C4, H4, C5 and H5 (324, 99, -121 and 92 mE, respectively) were calculated using NEMESIS (version 1.1, Oxford Molecular) and adjusted to give the same total charge in the zebularine pyrimidine ring to that of cytosine; the AMBER atom types CA and HA were chosen for C4 and H4, respectively, and a few standard bond angle parameters (available on request) were added to accommodate these atom types in the pyrimidine ring.

Results

The optimal nucleotide concentration range was determined to be 0.01mM to 10mM dNTP for our pyrosequencing-based assay. Concentrations higher than 10mM showed a plateau in signal (data not shown), with similar increases in control and experimental reactions, likely due to saturation of the system. Concentrations below 0.01mM showed virtually no detectable signal above background. Due to the nature of the enzymatic cascade, it is not possible to accurately assess the incorporation of dATP, as it can directly be used by the sulfurylase as an alternative substrate to ATP in generating the detected light signal (29). No appreciable signal or titration was observed for the incorporation of any other dNTPs opposite the thymidine template (table 1).

Incorporation opposite Adenine

dCTP did not show notable incorporation opposite adenine, as expected (Table 1). Similarly, dZTP, despite lacking a 4-amino group, behaved like dCTP and showed no detectable incorporation opposite adenine. Likewise, dGTP showed no pairing with A. dTTP, as expected,

was incorporated readily with a K_m/V_{max} =1.79x10^{-10} s^{-1} Incorporation of dUTP also occurred slightly less effectively (K_m/V_{max} =1x10^{-9} s^{-1}). Neither ara-dCTP nor d5mCTP showed notable incorporation.

Incorporation opposite Cytosine

Neither dCTP demonstrated significant incorporation opposite a cytosine template, as would be expected between homologous bases. Conversely, a high titratable signal was obtained for the incorporation of dGTP opposite cytosine (K_m/V_{max} =3.14x10^{-10} s^{-1}); the next base in the template strand is also a C, resulting in a higher signal for the incorporation of dGTP than the other favorable nucleotide pairings, due to a sequential extension by two bases rather than only one (refer to methods for template sequence). No notable signal was obtained for the incorporation of any of the other standard and non-standard nucleotides against C in the template (Table 1).

Incorporation opposite Guanine

dCTP was incorporated opposite G (K_m/V_{max}= 1.48x10^{-10} s^{-1}) similarly to the dNTPs in the other standard pairings (table 1). A similar, albeit slightly higher, signal was obtained for the incorporation of dZTP relative to dCTP (K_m/V_{max} =9.84x10^{-10} s^{-1}), demonstrating that dZTP acts as a dCTP analog despite lacking the 4-amino group present on cytosine. The extent of dZTP incorporation varied with the concentration of nucleotide injected. The higher the concentration of dZTP used, the greater was the signal produced relative to dCTP (data not shown); as at concentrations <10mM,, dCTP produced a slightly higher signal, indicating that the slightly better utilization of dZTP as a substrate based on a lower K_m/V_{max} for dZTP, obtained herein, may vary depending on the dZTP concentration evaluated. The pyrosequencer injects 0.5

microliters of dNTP solution into a 12 µl reaction volume, and therefore the approximate reaction concentrations of dZTP are 0.004mM, 0.04mM, 0.4mM and 4mM respectively. Previous estimates of intracellular dNTP pools range from 0.01mM to 0.213mM, and are within the range of our in vitro assay (34). d5mCTP, which possesses a 4-amino group, was incorporated opposite guanine (K_m/V_{max} =6.79x10^{-9} s^{-1}) less effectively than the unmethylated form, indicating some steric inhibition may exist; It is important to note that the 5 position of the pyrimidine ring is not involved in hydrogen bonding between G:C or A:T in Watson and Crick base pairing. Our assay also indicated that ara-dCTP is incorporated (K_m/V_{max} =1.99x10^{-10} s^{-1}) less readily than dCTP (Table 1).

Incorporation opposite Hypoxanthine

dCTP appears to incorporate well opposite the guanine analogue hypoxanthine (K_m/V_{max}=1.18x10^{-10} s^{-1}). However, dZTP was utilized less effectively (K_m/V_{max}=3.46x10^{-9} s^{-1}) than either dCTP or d5mCTP; therefore, although dZTP is effective as a dCTP analog when incorporated opposite G, this does not appear to be the case for incorporation opposite hypoxanthine (HX). This may be attributable to differences in hydrogen bonding between bases. A C:HX base pair is expected to form 2 hydrogen bonds, whereas a Z:HX pair can only form a single hydrogen bond, which may affect the stability of the base pair and the incorporation efficiency or rate of primer extension. d5mCTP was incorporated opposite hypoxanthine (K_m/V_{max}=5.28x10^{-9} s^{-1}) more readily than dZTP, but somewhat less effectively than dCTP opposite guanine (Table 1).

Incorporation opposite Zebularine

Incorporation opposite Z was investigated by two methods. As performed with the standard bases, individual dNTPs were incorporated opposite a Z-containing oligonucleotide template. As expected, dGTP incorporated opposite Z more readily than dCTP or dZTP (Table 1). dZTP also did not incorporate readily opposite Z (K_m/V_{max}=2.93x10^{-8} s^{-1}). We were unable to obtain data for dATP incorporation due to the high background generated by dATP injection into the Pyrosequencer at high concentrations.

Incorporation of nucleotides opposite of Z was also studied using standard Pyrosequencing. The Pyrosequencer was programmed to treat the Z template site as a potential single nucleotide polymorphism and the relative incorporation of dTTP, dCTP, dGTP and dATP was measured. dGTP was most efficiently incorporated opposite a Z template, consistent with our previous results that Z acts as a C analog. Due to limitations of the method, these data should be viewed more qualitatively rather than quantitatively

Although dGTP is favored to pair with Z, zebularine is not a perfect cytosine analog when in the template strand. A significant decrease in signal was noted after dGTP incorporation opposite of Z, which reflects a termination of oligonucleotide extension. In order to investigate this finding further, the standard oligonucleotide primer-template duplex was changed so Z was not the initial template base. The complementary oligonucleotide used to hybridize with the template oligonucleotide was shortened to allow the incorporation of 6 bases prior to reaching the Z template target base. In addition, the oligonucleotide allowed 11 bases to be incorporated after the Z template target base. With incorporation of each nucleotide triphosphate there is a small (average 6.5%) decrease in signal intensity, showing that there is not 100% efficiency in

extending all oligonucleotides. With incorporation of dGTP opposite Z there was a marked (53.2%) decrease in signal (data not shown). Therefore G is the preferred partner of Z when Z is in the template strand, but this Z:G pairing is not as efficient as C:G and A:T pairing in permitting chain extension when Z is in the template strand. This finding is unique to zebularine, since the identical experiment was performed with hypoxanthine in the template and no decrease in signal intensity was seen with dCTP incorporation opposite hypoxanthine (data not shown).

Computer Modeling

DNA structures formed after dZTP incorporation opposite cytosine, guanine, adenine and hypoxanthine are shown in Figure 3. As expected, two hydrogen bonds are present in the newly-formed G-Z base pair (Figure 3A), and one hydrogen bond is present in the HX-Z base pair (Figure 3D). This is reflected in the AMBER8 energies for the DNA structures containing the G-Z and HX-Z pairs (Table 2), which show the former structure to be more stable. Incorporation of dZTP opposite adenine (Figure 3B) results in a skewed conformation of the zebularine nucleotide, since no A-Z hydrogen bond formation can occur. Incorporation of dZTP opposite cytosine (Figure 3C) results in formation of a weak interaction between the cytosine 4-amino group and N3 of zebularine, but this requires twisting of dZTP and subsequent disruption of the developing duplex structure. Incorporation of dCTP opposite guanine (to give a normal Watson-Crick G-C pair) resulted in a structure that was more stable than the structure containing the G-Z pair (Table 2). This suggests that something other than the energetics of the newly-formed base pair accounts for the increased incorporation of dZTP opposite guanine, compared to dCTP. A similar behavior has been observed when other nucleoside analogs (35) and non-polar isosteres

of nucleobases (36) were incorporated into DNA, indicating that the geometry rather than thermodynamic stability is important for DNA polymerase activity.

For zebularine-containing templates, incorporation of dGTP opposite Z is energetically favorable, compared to the other dNTPs (Table 2), which is consistent with the experimental data and is a result of the two hydrogen bonds formed in the Z-G base pair (Figure 4A). The energies for incorporation of dATP, dTTP and dCTP opposite Z are similar, but it is perhaps of note that a hydrogen bond forms in the Z-A and Z-T base pairs (Figure 4B and 4D, respectively). These interactions are between N3 of zebularine with the 6-amino group of adenine and N3-H of thymine respectively. Both require some skewing of the base pair, which may compromise further chain extension. In contrast, incorporation of dCTP opposite Z does not result in a hydrogen bond between the Z and C bases; the distance between zebularine N3 and the cytosine 4-amino group (Figure 4C) is over 4 Å. These data support and offer an explanation for the experimental data, which show that both dATP and dTTP can incorporate opposite Z with low efficiency, but dCTP cannot incorporate opposite Z.

Discussion

We have shown that zebularine is utilized more effectively as a substrate for incorporation into DNA as a cytosine analogue, than as a thymine analogue. Our data also show that zebularine shows a greater degree of incorporation than ara-dCTP opposite both guanine and hypoxanthine, and that, in comparison with cytosine, zebularine is utilized less readily for incorporation opposite hypoxanthine

The pyrosequencing assay has inherent limitations due to the use of the exonuclease-deficient Klenow fragment of *Escherichia coli*, which lacks the proofreading activity that would be present in an *in vivo* model, as well as the eukaryotic polymerase active in human cancer cells. However, previous studies have shown this to be a solid foundational model system to elucidate the basic mechanism of DNA incorporation and polymerase specificity (37), our primary goal in this study. In addition, similar nucleotide selectivity for Klenow and DNA polymerase alpha has been demonstrated(38). Additionally, the quantitative variability of the enzyme system produces a relatively high degree of scatter, demonstrated in the relatively large standard deviation values (table 1). Thus the values of Km/V determined are reflective of a relative degree of enzyme activity within this assay, and useful for side-by-side comparison of and not a precise calculation of the Km/V.

Zebularine was utilized as a cytosine analog (Figure 1A&D). This is surprising given the absence of the NH_2 group at the 4 position of the pyrimidine ring, which results in one less hydrogen bond for the G:Z pairing relative to the G:C pairing (Figures 3A and 4A). Such a high degree of incorporation suggests effective recognition by the polymerase when bound to the primed template G. This supports the role of zebularine as a demethylating agent and potential chemotherapeutic, because in order to block the activity of DNA methyltransferase, zebularine must first be specifically incorporated into DNA in place of cytosine (21, 39).

We observed that zebularine has no significant incorporation opposite A. Although the lack of a 4-amino group on zebularine removes one repulsive force to mismatch pairing with A, there are no compatible hydrogen bond acceptors or donors to promote interaction with A (Figure 3B).

The only structural similarity to thymine or uracil is the absence of the 4-amino group (Figure 1D, E&F), but the lack of a carbonyl group at the 4-position is apparently sufficient to distinguish Z from T and U and prevent any appreciable incorporation. Similarly there is no significant incorporation opposite either thymine or cytosine, further supporting the hypothesis that dZTP is utilized efficiently in place of dCTP. This result is significant since dZTP has previously been shown to be a weaker inhibitor of DNA methylation than 5-aza-dCTP(15). One possible explanation, that dZTP is misincorporated in place of dTTP, thus mitigating its potency, is therefore excluded based on our observations.

Although both dCTP and 5mdCTP are utilized effectively for incorporation opposite guanine and hypoxanthine , we observed a significant drop in the ability for dZTP to be used as a substrate when incorporated opposite hypoxanthine relative to dCTP and 5mdCTP (Table 1). This may be due to the decrease in hydrogen bonding sites in the hypoxanthine pairing relative to guanine. For both dCTP and 5mdCTP, there are three sites available for hydrogen bonding on guanine and two on hypoxanthine. In the case of dZTP, the lack of a 4-amino group reduces the number of sites to one in pairing to hypoxanthine (Figure 3D). Since a similar signal was observed for the incorporation of dCTP/d5mCTP opposite guanine and hypoxanthine, it seems a pairing with two hydrogen bond sites has a similar rate of incorporation to that of a pairing with three sites. Thus the incorporation of dZTP opposite guanine occurs as readily as dCTP. However a drop to one available hydrogen bond (in the case of the Z-HX pairing) may decrease the stability of the complex and thus the rate of incorporation, explaining the reduced signal that we observed. Further studies using other modified pyrimidine base analogues would be necessary to confirm this hypothesis.

Z in the template strand behaves again as a C analog and most effective substrate utilization occurs with dGTP. However, there is a low level of mispairing with dATP and to a lesser degree with dTTP. This is consistent with earlier mutational studies. A high rate of C to T mutations in *Escherichia coli* treated with zebularine may be the result of A:Z misincorporation during subsequent rounds of replication after dZTP has been incorporated into DNA (40). Although when in the template strand Z prefers to pair with G, there is a significant decrease in nucleotide incorporation opposite Z. This phenomenon is unique to Z and is not seen with C pairing opposite HX. Both Z:G and HX:C pairs include two hydrogen bonds compared to the three hydrogen bonds between C:G, and therefore, this chain termination is likely to be independent of the decreased hydrogen bonding between Z:G. It has previously been reported that zebularine in the template strand leads to a direct block in DNA replication(41). The effect of zebularine incorporation into the template deserves further study as this propensity for misincorporation and inhibition of DNA replication may eventually play a role in its chemotherapeutic effect.

Acknowledgements

A.S.Y. is the recipient of a STOP Cancer Career Development Award and the T.Franklin Williams Scholars-American Society of Oncology Career Development Award. This work was sponsored in part by a grant from the Wright Foundation.

References

1. Jones, P.A., Baylin, S.B. 2002. The fundamental role of epigenetic events in cancer, *Nature Reviews Genetics*, **3**(6), 415-28.

2. Bestor, T.H., Verdine, G.L. 1994. DNA methyltransferases, *Current Opinion in Cell Biology*, **6**(3), 380-9.

3. Klimasauskas, S., Kumar, S., Roberts, R.J., Cheng, X. 1994. HhaI methyltransferase flips its target base out of the DNA helix.[see comment]. *Cell*, **76**(2), 357-69.

4. Wu, J.C., Santi, D.V. 1987. Kinetic and catalytic mechanism of HhaI methyltransferase, *Journal of Biological Chemistry*, **262**(10), 4778-86.

5. Smith, S.S., Kaplan, B.E., Sowers, L.C., Newman, E.M. 1992. Mechanism of human methyl-directed DNA methyltransferase and the fidelity of cytosine methylation, *Proceedings of the National Academy of Sciences of the United States of America*, **89**(10), 4744-8.

6. Brank, A.S., Eritja, R., Garcia, R.G., Marquez, V.E., Christman, J.K. 2002. Inhibition of HhaI DNA (Cytosine-C5) methyltransferase by oligodeoxyribonucleotides containing 5-aza-2'-deoxycytidine: examination of the intertwined roles of co-factor, target, transition state structure and enzyme conformation. *Journal of Molecular Biology*, **323**(1), 53-67.

7. Christman, J.K. 2002. 5-Azacytidine and 5-aza-2'-deoxycytidine as inhibitors of DNA methylation: mechanistic studies and their implications for cancer therapy, *Oncogene*, 21(35), 5483-95.

8. Jones, P.A., Taylor, S.M. 1980. Cellular differentiation, cytidine analogs and DNA methylation, *Cell*, **20**(1), 85-93.

9. Glover, A.B., Leyland-Jones, B.R., Chun, H.G., Davies, B., Hoth, D.F. 1987. Azacitidine: 10 years later, *Cancer Treatment Reports*, **71**(7-8), 737-46.

10. Gilbert, J., Gore, S.D., Herman, J.G., Carducci, M.A. 2004. The clinical application of targeting cancer through histone acetylation and hypomethylation, *Clinical Cancer Research*,**10**(14), 4589-96.

11. Santini, V., Kantarjian, H.M., Issa, J.P. 2001. Changes in DNA methylation in neoplasia: pathophysiology and therapeutic implications, *Annals of Internal Medicine*,**134**(7), 573-86.

12. Silverman, L.R., Demakos, E.P., Peterson, B.L., *et al*. 2002. Randomized controlled trial of azacitidine in patients with the myelodysplastic syndrome: a study of the cancer and leukemia group B.[see comment], *Journal of Clinical Oncology*, **20**(10):2429-40.

13. Wijermans, P., Lubbert, M., Verhoef, G., *et al*. 2000. Low-dose 5-aza-2'-deoxycytidine, a DNA hypomethylating agent, for the treatment of high-risk myelodysplastic syndrome: a multicenter phase II study in elderly patients, *Journal of Clinical Oncology,* **18**(5):956-62.

14. Issa, J.-P.J., Garcia-Manero, G., Giles, F.J., *et al*. 2004. Phase 1 study of low-dose prolonged exposure schedules of the hypomethylating agent 5-aza-2'-deoxycytidine (decitabine) in hematopoietic malignancies, *Blood*, **103**(5),1635-40.

15. Cheng, J.C., Matsen, C.B., Gonzales, F.A., *et al*. 2003. Inhibition of DNA methylation and reactivation of silenced genes by zebularine, *J Natl Cancer Inst*, **95**(5):399-409.

16. Cheng, J.C., Weisenberger, D.J., Gonzales, F.A., *et al*. 2004. Continuous zebularine treatment effectively sustains demethylation in human bladder cancer cells, *Mol Cell Biol*,**24**(3):1270-8.

17. Holleran, J.L., Parise, R.A., Joseph, E., *et al*. 2005. Plasma pharmacokinetics, oral bioavailability, and interspecies scaling of the DNA methyltransferase inhibitor, zebularine, *Clinical Cancer Research*,**11**(10), 3862-8.

18. Klecker, R.W., Cysyk, R.L., Collins, J.M. 2006. Zebularine metabolism by aldehyde oxidase in hepatic cytosol from humans, monkeys, dogs, rats and mice: Influence of sex and inhibitors, *Bioorg Med Chem*,**14**, 62-6.

19. Zhou, L., Cheng, X., Connolly, B.A., Dickman, M.J., Hurd, P.J., Hornby, D.P. 2002. Zebularine: a novel DNA methylation inhibitor that forms a covalent complex with DNA methyltransferases, *J Mol Biol*, **321**(4):591-9.

20. Ford, K., Taylor, C., Connolly, B., Hornby, D.P. 1993. Effects of co-factor and deoxycytidine substituted oligonucleotides upon sequence-specific interactions between MspI DNA methyltransferase and DNA, *Journal of Molecular Biology*, **230**(3), 779-86.

21. Hurd, P.J., Whitmarsh, A.J., Baldwin, G.S., *et al*. 1999. Mechanism-based inhibition of C5-cytosine DNA methyltransferases by 2-H pyrimidinone, *J Mol Biol*, **286**(2), 389-401.

22. Marquez, V.E., Eritja. R., Kelley, J.A., Vanbemmel, D., Christman, J.K. 2003. Potent inhibition of HhaI DNA methylase by the aglycon of 2-(1H)-pyrimidinone riboside (zebularine) at the GCGC recognition domain, *Ann N Y Acad Sci*, **1002**,154-64.

23. Ben-Kasus, T., Ben-Zvi, Z., Marquez, V., Kelley, J., Agbaria, R. 2005. Metabolic activation of zebularine, a novel DNA methylation inhibitor, in human bladder carcinoma cells, *Biochem Pharmacol*, **70**,121-33.

24. Charczuk, R., Tamm, C., Suri, B., Bickle, T.A. 1986. An unusual base pairing between pyrimidine and pyridine nucleotides, *Nucleic Acids Research*, **14**(23), 9530.

25. Shen, J.C., Creighton, S., Jones, P.A., Goodman, M.F. 1992. A comparison of the fidelity of copying 5-methylcytosine and cytosine at a defined DNA template site, *Nucleic Acids Research*, **20**(19), 5119-25.

26. Vives, M., Eritja, R., Tauler, R., Marquez, V.E., Gargallo, R. 2004. Synthesis, stability, and protonation studies of a self-complementary dodecamer containing the modified nucleoside 2'-deoxyzebularine. Biopolymers, **73**(1), 27-43.

27. Barchi, J.J., Jr., Cooney, D.A., Hao, Z. *et al*. 1995. Improved synthesis of zebularine [1-(beta-D-ribofuranosyl)-dihydropyrimidin-2-one] nucleotides as inhibitors of human deoxycytidylate deaminase, *J Enzyme Inhib*, **9**(2), 147-62.

28. Ronaghi, M. 2001. Pyrosequencing sheds light on DNA sequencing. *Genome Res*, **11**(1), 3-11.

29. Ronaghi, M., Karamohamed, S., Pettersson, B., Uhlen, M., Nyren, P. 1996. Real-time DNA sequencing using detection of pyrophosphate release, *Anal Biochem*, **242**(1), 84-9.

30. Ahmadian, A., Gharizadeh, B., Gustafsson, A.C., et al. 2000. Single-nucleotide polymorphism analysis by pyrosequencing, *Anal Biochem*, **280**(1),103-10.

31. Ronaghi, M. 2003. Pyrosequencing for SNP genotyping, *Methods Mol Biol*, **212**, 189-95.

32. Chambers, E.J., Price, EA, Bayramyan MC, Haworth IS. 2003. Computation of DNA backbone conformations, *Journal of Biomolecular Structure & Dynamics* **21**(1), 111-25.

33. Case DA, Darden TA, Cheatham I, T.E., et al. 2004. AMBER 8. In. San Francisco: University of California.

34. Leeds, J.M., Slabaugh, M.B., Mathews, C.K. 1985. DNA precursor pools and ribonucleotide reductase activity: distribution between the nucleus and cytoplasm of mammalian cells, *Molecular & Cellular Biology*, **5**(12), 3443-50.

35. Eritja, R., Horowitz, D.M., Walker, P.A., et al. 1986. Synthesis and properties of oligonucleotides containing 2'-deoxynebularine and 2'-deoxyxanthosine, *Nucleic Acids Research*,**14**(20), 8135-53.

36. Kool, E.T. Morales, J.C., Guckian, K.M. 2000. Mimicking the structure and function of DNA: Insights into DNA stability and replication, *Angew Chem Int Ed*, **39**(6), 990-1009.

37. Chiaramonte, M., Moore, C.L., Kincaid, K., Kuchta, R.D. 2003. Facile polymerization of dNTPs bearing unnatural base analogues by DNA polymerase alpha and Klenow fragment (DNA polymerase I), *Biochemistry*, **42**(35),10472-81.

38. Shen, J.C., Creighton, S., Jones, P.A., Goodman, M.F. 1992. A comparison of the fidelity of copying 5-methylcytosine and cytosine at a defined DNA template site, *Nucleic Acids Res*, **20**(19), 5119-25.

39. Gowher, H., Jeltsch, A. 2004. Mechanism of inhibition of DNA methyltransferases by cytidine analogs in cancer therapy, *Cancer Biol Ther*, **3**(11):1062-8.

40. Lee, G., Wolff, E., Miller, JH. 2004. Mutagenicity of the cytidine analog zebularine in Escherichia coli, *DNA Repair* (Amst), 3(2), 155-61.

41. Charczuk, R., Tamm, C., Suri, B., Bickle, T.A. 1986. An unusual base pairing between pyrimidine and pyridine nucleotides, *Nucleic Acids Res*, **14**(23), 9530.

Figure Captions

Table 1: dNTP incorporation by Klenow fragment of DNA polymerase 1 opposite a variable template base in the sequence CTCAGTGTTAC**X**GTACATGGGTTCCTATTG using the Pyrosequencer reaction. Each value was determined through Lineweaver-Burke analysis of dNTP substrate concentration and Pyrosequencer peak height as a surrogate of reaction velocity Values are in s^{-1}.

Table 2: AMBER8 energies (kcal) for DNA duplexes containing zebularine.

[a] Energies for duplex d(CTCAGTGTTANXGTACATGGGTTCCTATTG). d(CAATAGGAACCCATGTACY), containing an 11-base overhang, 5′-OH and 3′-OH ends, and 47 sodium counterions included for neutrality.

Figure 3: The structures are viewed from the minor groove of the DNA duplex, and the template strand is on the left in each structure. The C-Z, A-Z, G-Z and HX-Z pairs are identified, and the hydrogen bonds formed in the G-Z pair (two hydrogen bonds) and HX-Z pair (one hydrogen bond) are indicated by green dots.

Figure 4: The structures are viewed from the minor groove of the DNA duplex, and the template strand is on the left in each structure. The Z-G, Z-A, Z-C and Z-T pairs are identified, and the hydrogen bonds formed in the Z-G pair (two hydrogen bonds), Z-A (one hydrogen bond), and Z-T pair (one hydrogen bond) are indicated by green dots.

Table 1: Extrapolated K_m/V_{max} values (in s^{-1} units) calculated from Pyroseqencing by utilizing the signal intensity over a constant time interval as a surrogate for reaction velocity.

	dCTP	**dGTP**	**dTTP**	**dZTP**	**dUTP**	**Ara-dCTP**	**5m-dCTP**
A	$4.39X10^{-9} \pm 1.2X10^{-9}$	$1.74X10^{-9} \pm 1.41X10^{-10}$	$1.79X10^{-10} \pm 2.16X10^{-12}$	$1.24_{X10}{}^{-8} \pm 1.61X10^{-9}$	$1.00X10^{-9} \pm 3.84X10^{-11}$	$1.64X10^{-8} \pm 3.90X10^{-10}$	$8.12X10^{-9} \pm 2.76X10^{-9}$
C	$3.30X10^{-9} \pm 8.50X10^{-10}$	$3.14X10^{-10} \pm 7.61X10^{-12}$	$4.25X10^{-9} \pm 2.55X10^{-10}$	$1.44X10^{-8} \pm 3.53X10^{-9}$	$1.38X10^{-8} \pm 3.33X10^{-9}$	$5.51X10^{-9} \pm 2.37X10^{-10}$	$6.50X10^{-9} \pm 1.10X10^{-9}$
G	$1.48X10^{-10} \pm 1.40X10^{-11}$	$1.84X10^{-8} \pm 1.25X10^{-8}$	$7.82X10^{-9} \pm 1.36X10^{-9}$	$2.09X10^{-9} \pm 2.21X10^{-10}$	$2.65X10^{-8} \pm 2.82X10^{-9}$	$1.99X10^{-10} \pm 1.81X10^{-9}$	$6.79X10^{-9} \pm 7.55X10^{-12}$
T	$1.37X10^{-9} \pm 8.00X10^{-10}$	$1.74X10^{-9} \pm 1.41X10^{-10}$	$1.10X10^{-8} \pm 3.21X10^{-9}$	$9.59X10^{-9} \pm 2.11X10^{-9}$	$2.92X10^{-8} \pm 7.62X10^{-9}$	$8.18X10^{-9} \pm 1.58X10^{-9}$	$8.59X10^{-9} \pm 1.94X10^{-10}$
I	$1.18X10^{-10} \pm 3.30X10^{-11}$	$2.12X10^{-9\backslash} \pm 1.58X10^{-10}$	$4.11X10^{-9} \pm 1.40X10^{-9}$	$3.46X10^{-9} \pm 1.04X10^{-9}$	$3.60X10^{-8} \pm 1.25X10^{-8}$	$2.30X10^{-10} \pm 2.29X10^{-9}$	$5.28X10^{-9} \pm 5.49X10^{-12}$
Z	$9.84X10^{-9} \pm 2.50X10^{-9}$	$2.19X10^{-10} \pm 9.84X10^{-13}$	ND	$2.93X10^{-8} \pm 3.27X10^{-9}$	ND	ND	ND

ND-Study not done

Table 2: AMBER8 energies for the DNA structures containing different base pairs

X-Y [a]	Energy	X-Y [a]	Energy
C-G	-861.8	I-C	-846.8
C-Z	-842.4	I-Z	-834.0
A-T	-848.4	Z-A	-837.6
A-Z	-837.2	Z-T	-839.8
G-C	-864.4	Z-C	-839.4
G-Z	-846.4	Z-G	-850.4

N = C for X ≠ Z and N=G for X = Z.

Figure 1: Structure of various nucleotide analogs.

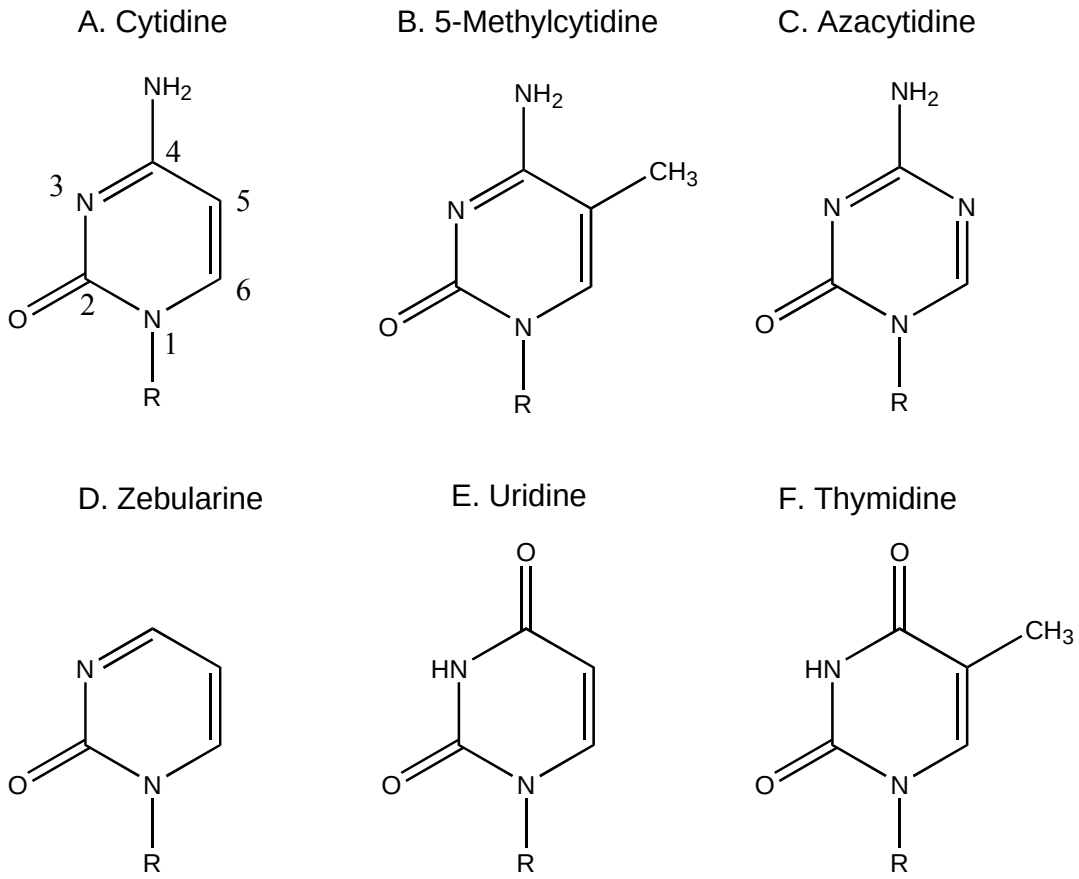

R=ribose, deoxyribose, or deoxyribose triphosphate. (A) Cytosine, (B) 5-Methylcytosine, (C) Azacytosine (if R=ribose then azacytidine; if R=deoxyribose then decitabine), (D) Zebularine, (E) Uracil, and (F) Thymine

Figure 2: Schema showing the hybridized oligonucleotide template used in our Pyrosequencing assay.

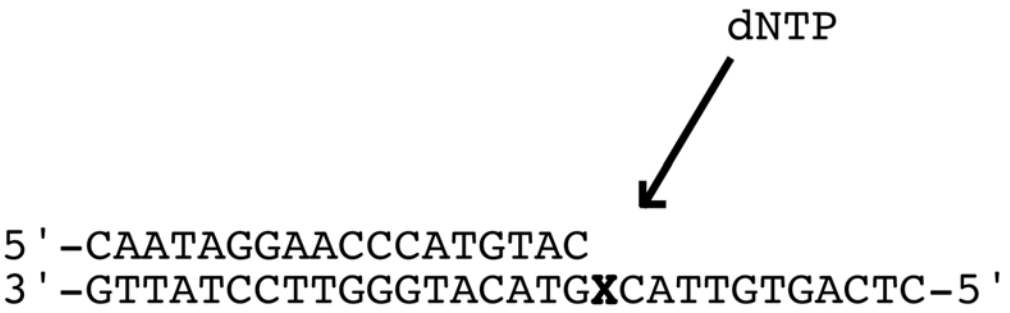

X=variable base (A, C, G, T, or Z). Incorporation of various nucleotide triphosphates, dNTP, was studied by Pyrosequencing.

Figure 3: Energy-minimized primer-template DNA structures following dZTP incorporation opposite (A) guanine, (B) adenine, (C) cytosine and (D) hypoxanthine.

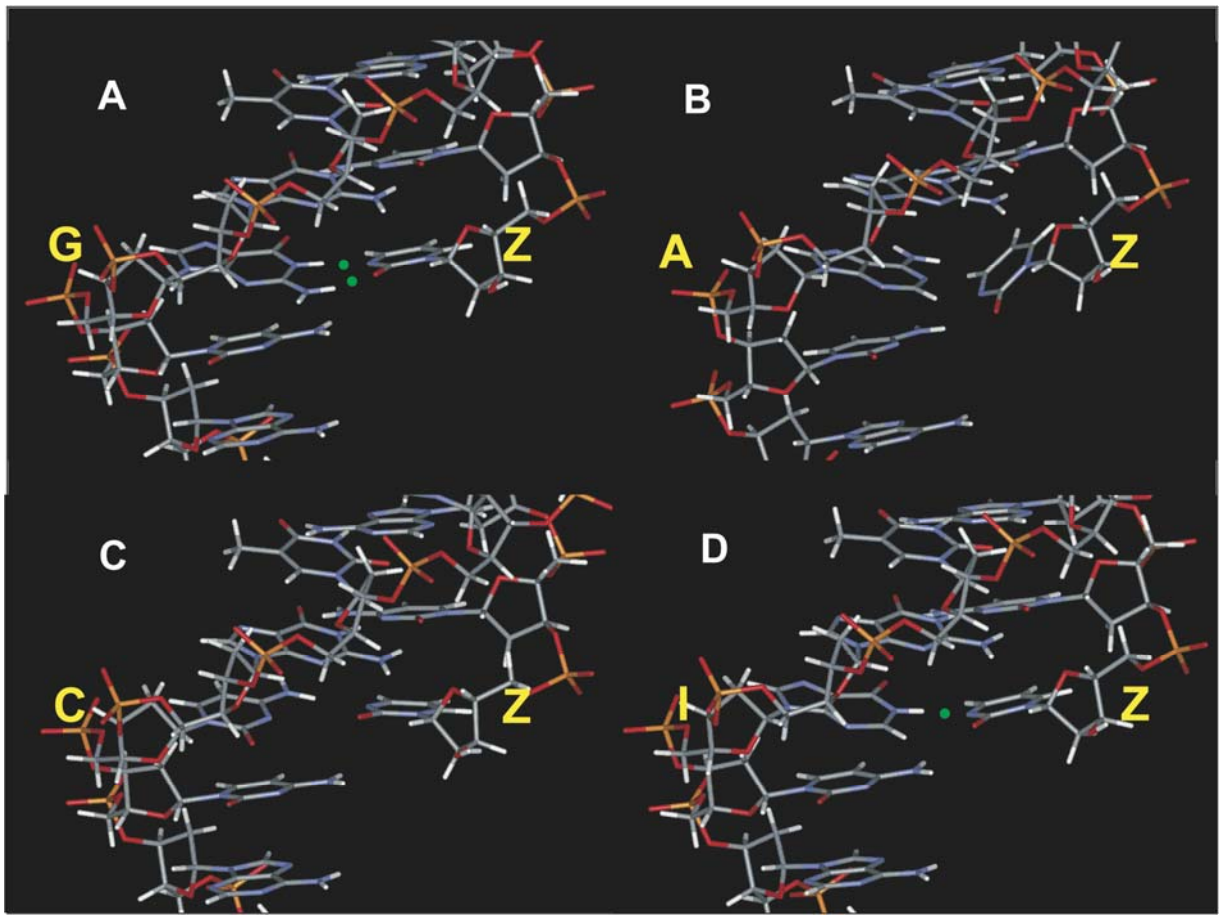

Figure 4: Energy-minimized primer-template DNA structures following dNTP incorporation opposite zebularine. (A) dGTP, (B) dATP, (C) dCTP, and (D) dTTP.